European Review for Medical and Pharmacological Sciences 2018; 22: 1094-1101

A volumetric intracoronary ultrasonographic study of coronary bifurcation lesions

Q.-H. LI, Q. ZHANG, X.-L. LI, J.-F. YIN, H.-G. JI

Department of Cardiology, Changzhou TCM Hospital, Changzhou, Jiangsu Province, China

Abstract. – OBJECTIVE: To evaluate the plaque distribution and composition pattern in the left main coronary artery (LMCA) disease using intracoronary ultrasound.

PATIENTS AND METHODS: Intravascular ultrasound data of 50 patients from the January 2010 to December 2015 with significant LMCA bifurcation lesions, with angiographic diameter stenosis >50%, and requiring revascularization, were evaluated. Plaque burden and percentage of necrotic core (% NC) at the minimal lumen area site and maximal % NC site were measured in different segments. The segments that were included in the study are as follows: segment 1: proximal LMCA, segment 2: left anterior descending (LAD) ostium, segment 3: left circumflex branch (LCX) ostium, segment 4: proximal LAD, segment 5: proximal LCX. According to its relationship with the bifurcation ridge, the blood vessel wall was divided into the contralateral bifurcation ridge blood vessel wall and bifurcation ridge blood vessel wall.

RESULTS: Plaque burden results showed that the plaque eccentricity index of segment 2 and segment 3 was significantly higher than that of the other segments at sites of the minimal lumen area and maximal % NC with a statistically significant difference ($p<0.05$). Plaque eccentricity index of contralateral bifurcation ridge was significantly higher than that of the bifurcation ridge, and the difference was statistically significant ($p<0.05$). Analysis of plaque composition showed the fibrous tissue percentage of segment 2 and segment 3 was significantly higher than the other segments that at the sites of minimal lumen area and the maximal % NC site. The fibrous percentage of the contralateral bifurcation ridge was significantly lower than that of the bifurcation ridge.

CONCLUSIONS: Intravascular ultrasound is an effective way for detecting the distribution and composition of the atherosclerotic plaque at the left main coronary artery bifurcation and is of great significance to adjuvant interventional therapy.

Key Words:

Intracoronary ultrasound, LMCA, Bifurcation disease, Plaque distribution, Lumen area.

Introduction

Left main coronary artery is the main blood supply to the left heart muscle. It is divided into the left anterior descending artery and left circumflex artery, forming a y-shaped arterial bifurcation. When blood flows through the bifurcation, there will be a change in the hemodynamics mechanism. This change leads to more easily formation of atherosclerotic plaques in this area, causing arterial stenosis and further leads to the left main bifurcation lesions[1-3]. Interventional therapy is currently the main approach to treat the coronary stenosis caused by coronary atherosclerotic plaques[4]. The appropriate intervention strategy is required for the identification of plaque characteristics. Conventional coronary angiography cannot accurately assess the position and plaques characteristic[5]. So, in recent years, rapidly developed intravascular ultrasound (IVUS) technology performed in the implementation of plaque characteristic determination[6,7]. Further, intervention can be guided according to the characteristics[8,9]. So, with this in mind, we have evaluated the application of intravascular ultrasound in left main coronary artery disease, which assesses the characteristics of the plaques in order to carry out further treatments.

Patients and Methods

Patients diagnosed with coronary artery disease and completed coronary angiography in the Department of Cardiology at Changzhou TCM Hospital (Jiangsu Province, China) were taken as study samples. All the patients were selected from January 2010 to December 2015. Total sample size comprised of 50 patients, including 32 males and 18 females. This investigation was approved by the Ethics Committee of Changzhou TCM Hospital (Jiangsu Province, China). Signed written informed consents were obtained from all partici-

Corresponding Author: Yan Bai, MD; e-mail: yanbaiaas@126.com

pants before the study. The inclusion criteria were: (1) patients first diagnosed with stable angina or acute coronary syndrome; (2) in-hospital coronary angiography revealed left main-LAD/LCX bifurcation lesions (stenosis >50%); (3) patient and the family members signed an agreement on IVUS examination. The exclusion criteria were: (1) ultrasound images obtained cannot be accurately measured or analyzed; (2) the left main coronary artery was too short to be examined.

IVUS examination: first of all, the femoral artery was conventionally punctured and IVUS catheter was placed. The IVUS catheter (Boston Scientific Corporation, Boston, MA, USA) AtlantisTM (3.0 Fr, 40 MHz) was used for the procedure. The probe used was of monorail mechanical rotation type with automatic retraction at the speed of 0.5 mm/s with image acquisition speed of 30 frames/s. The operating system was GalaxyTM (Boston Scientific (Boston, MA, USA). IVUS catheter was placed onto the lesion, image acquisition system was connected, and Real-time imaging and recording were performed.

Ultrasound image analysis: LMCA lesions were divided into 5 segments according to the distance to the bifurcation site: proximal LMCA, segment 2: left anterior descending (LAD) ostium, segment 3: left circumflex branch (LCX) ostium, segment 4: proximal LAD, segment 5: proximal LCX (Figure 1). According to the relationship with the bifurcation, the vessel wall was divided into the bifurcation ridge vessel wall and the contralateral bifurcation ridge vessel wall. The cross-sectional area of the external elastic membrane and the lumen were measured at the site of minimum lumen area of each segment. The plaque area, plaque burden, and plaque eccentricity index were measured by the following formulas:

- Plaque area = external elastic membrane cross-sectional area – lumen cross-sectional area.
- Plaque burden = plaque area/external elastic membrane cross-sectional area.
- Plaque eccentricity index = maximum plaque and media thickness/minimum plaque and media thickness.

Measurement of the intra-plaque tissue structure: the area of fibrous tissue, fibrous lipid, calcified tissue and necrotic core at the minimum lumen area and the maximum necrotic core were measured; the percentage of the total area was calculated according to the area percentage of each part.

Statistical Analysis

SPSS 17.0 (SPSS Inc., Chicago, IL, USA) was used for the statistical analysis. Measurement data were expressed as mean ± standard deviation. Two independent samples t-test were used for the comparison between the two groups. Enumeration data were expressed as the number of cases (percentage), $\chi 2$-test was performed for the comparison between the two groups. p-value<0.05 for the difference was considered as statistically significant results.

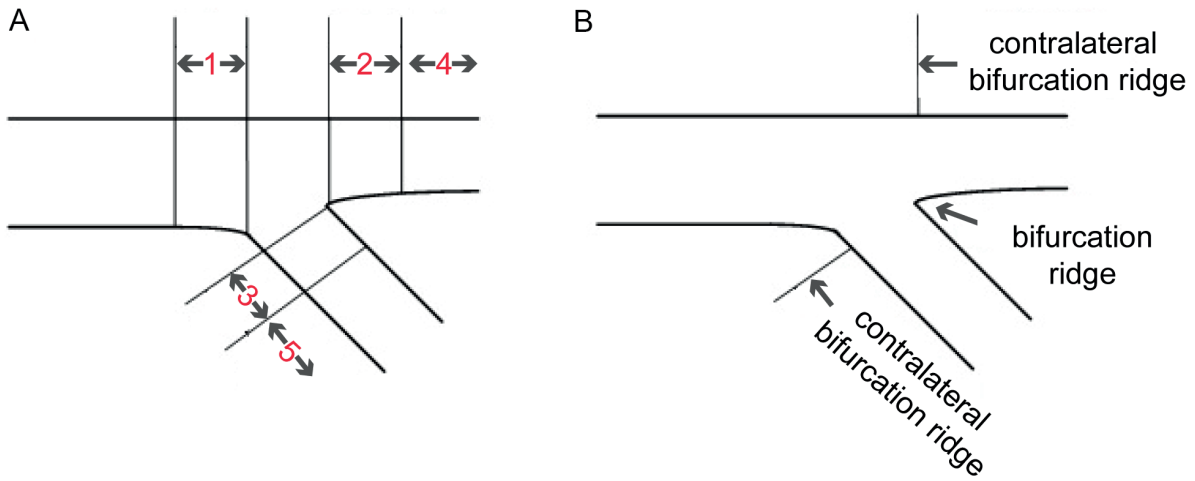

Figure 1. A schematic diagram of LMCA bifurcation lesion (the left figure was divided into 5 segments; the right figure was divided into 2 areas).

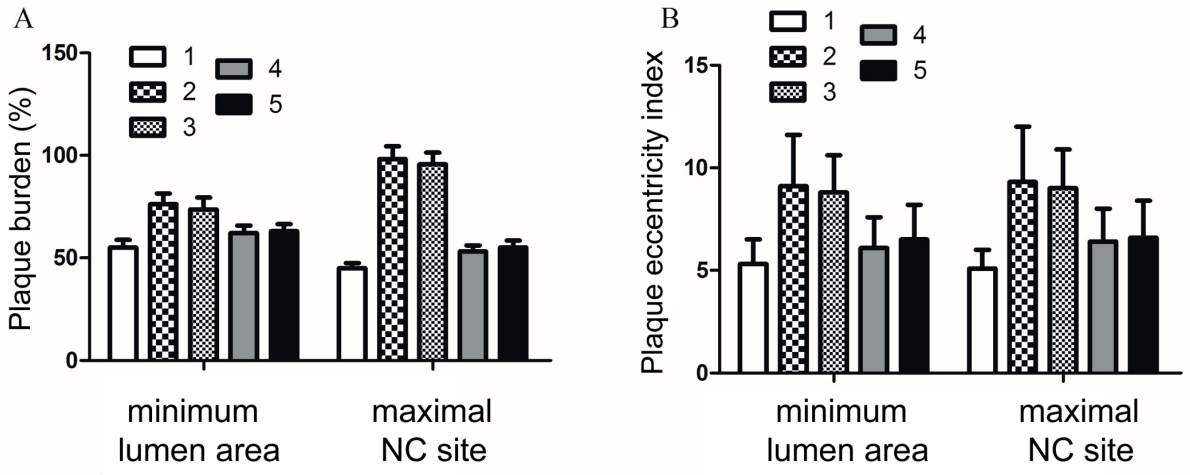

Figure 2. Analysis of the plaque at the minimum lumen area site and the maximal % NC site in the all the five segments of LMCA bifurcation. ***A,*** Plaque burden; ***B,*** Plaque eccentricity index. Intravascular ultrasound showed that the plaque burden and plaque eccentricity index of segment 2 and 3 of the LMCA bifurcation were significantly higher than that of the other segments at the minimum lumen area site and the maximal % NC site.

Results

Clinical Data

50 patients were included in this study, which includes 32 males (64%), 18 females (36%) with the average age of 67.2±7.9 years. The disease history and Medina classification of all selected patients were listed in Table I.

Analysis of LMCA bifurcation plaque burden: the analytic result of the all the five segments revealed the plaque burden at the site of minimum lumen area was as followed: segment 1 (55.1±3.7)%, segment 2 (76.2±5.2)%, segment 3 (73.7±5.7)%, segment 4 (62.2±3.6)%, segment 5 (63.1±3.4)%. The multiple comparison results showed that the plaque burden of segment 2 and 3 was significantly higher than that of the other segments and the difference was statistically significant (p-value <0.05). The plaque eccentricity index of all the five segments was: segment 1 (5.3±1.2), segment 2 (9.1±2.5), segment 3 (8.8±1.8), segment 4 (6.1±1.5), segment 5 (6.5±1.7). The multiple comparison results showed that the plaque eccentricity index of

Table I. Clinical data of study object.

	mean ± standard deviation/number of cases (%)
Age, years	67.2±7.9
Gender, number of cases (%)	
Male	32 (64)
Female	18 (36)
Hypertension history,number of cases (%)	45 (90)
Diabetes history, number of cases (%)	21 (42)
Hyperlipidemia, number of cases (%)	40 (80)
Stable angina, number of cases (%)	37 (74)
Acute coronary syndrome, number of cases (%)	13 (26)
Angle of bifurcation, degree	55.2±19.4
Medina classification, number of cases (%)	
(0,0,1)	2 (4)
(0,1,0)	8 (16)
(0,1,1)	3 (6)
(1,0,0)	3 (6)
(1,0,1)	4 (8)
(1,1,0)	11 (22)
(1,1,1)	19 (38)

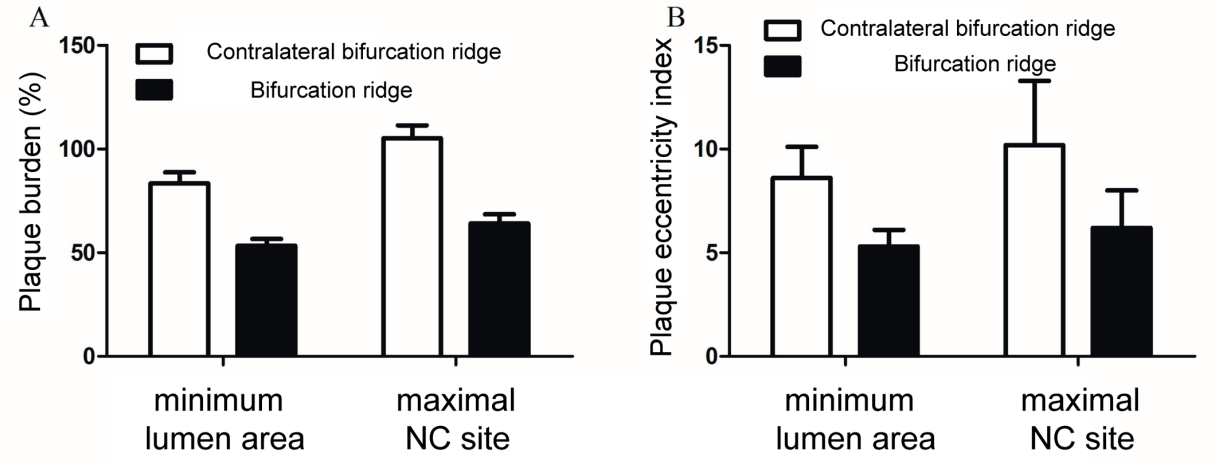

Figure 3. Comparison of LMCA bifurcation ridge and contralateral bifurcation ridge at minimum lumen area site and maximal % NC site. ***A,*** Plaque burden; ***B,*** Plaque eccentricity index. Intravascular ultrasound showed the plaque burden and the plaque eccentricity index of the LMCA contralateral bifurcation ridge was significantly higher than at of the LMCA bifurcation ridge at the minimal lumen area site and the maximal % NC site.

segment 2 and 3 were significantly higher than that of the other segments and the difference was statistically significant (p-value <0.05). The plaque burden of all five segments at the maximal percentage of necrotic core (% NC) site was: segment 1 (45.1±2.5)%, segment 2 (98.3±6.1)%, segment 3 (95.7±5.7)%, segment 4 (53.2±2.8)%, segment 5 (55.2±3.3)%. The multiple comparison results showed that the plaque burden of segment 2 and 3 was significantly higher than that of the other segments and the difference was statistically significant (p-value <0.05). The plaque eccentricity index of all the five segments was: segment 1 (5.1±0.9), segment 2 (9.3±2.7), segment 3 (9.0±1.9), segment 4 (6.4±1.6), segment 5 (6.6±1.8). The multiple comparison results showed that the plaque eccentricity index of segment 2 and 3 were significantly higher than that of the other segments and the difference was statistically significant (p-value <0.05) (Figure 2). In left main bifurcation lesions, at the minimum lumen area site, the plaque burden of the contralateral bifurcation ridge was significantly higher than the plaque burden of the bifurcation ridge (83.4±5.4 vs. 53.3±3.4). The multiple comparison results showed statistically significant p-value of <0.05. The plaque eccentricity index of the contralateral bifurcation ridge was significantly higher than the plaque eccentricity index of the bifurcation ridge (8.6±1.5 vs. 5.3±F0.8). The multiple comparison results showed statistically significant p-value of <0.05. At the maximal % NC site, the plaque burden of the contralateral bifurcation ridge was also significantly higher than the plaque burden of the bifurcation ridge (105.2±6.2 vs. 64.1±4.4). The multiple comparison results showed statistically significant p-value of <0.05. The plaque eccentricity index of the contralateral bifurcation ridge was significantly higher than the plaque eccentricity index of the bifurcation ridge (10.2±3.1 vs. 6.2±1.8). The multiple comparison results showed statistically significant p-value of <0.05 (Figure 3).

Analysis of LMCA bifurcation plaque tissue structure: at the minimum lumen area site from the segment 1 to 5, the fibrous tissue percentage was: 63.9±3.5, 48.3±2.2, 49.5±2.5, 58.9±3.1, 60.1±3.2, respectively. At the minimum lumen area site from the segment 1 to 5, the fibrous lipid tissue percentage was 11.1±1.2, 8.1±1.1, 8.7±1.2, 9.8±0.9, 10.8±1.1, respectively. At the minimum lumen area site from the segment 1 to 5, the calcified tissue percentage was: 10.1±1.1, 19.4±2.1, 18.1±1.8, 15.2±1.3, 14.5±1.1, respectively; the necrotic core percentage was 15.2±1.4, 25.4±2.0, 24.5±2.1, 17.1±1.5, 16.5±1.6, respectively. Multiple comparison results showed that the fibrous tissue percentage of segment 2 and 3 was significantly lower than that of the other segments. The % NC was significantly higher than that of the other segments, the differences were statistically significant (p<0.05). The fibrous tissue percentage of contralateral bifurcation ridge plaques was 50.1±2.3, fibrous lipid tissue percentage was 8.9±1.1, calcified tissue percentage was 18.8±1.8, % NC was 23.8±1.9. The fibrous tissue percentage

of bifurcation ridge plaques was 61.2±3.1, fibrous lipid tissue percentage was 10.2±1.1, calcified tissue percentage was 14.3±1.1, and % NC was 15.5±1.2. The contralateral bifurcation ridge had lower fibrous tissue percentage and higher % NC than the bifurcation ridge. The differences were statistically significant (p<0.05) (Figures 4 and 5). At the maximal % NC site from segment 1 to 5, the fibrous tissue percentage was: 53.6±3.3, 39.3±1.8, 40.1±2.0, 49.8±2.1, 50.4±2.5, respectively. At the maximal % NC site from segment 1 to 5, fibrous lipid tissue percentage was 6.6±0.7, 3.7±0.5, 4.0±0.8, 5.0±0.9, 6.0±0.9, respectively. At the maximal % NC site from segment 1 to 5, calcified tissue percentage was: 13.2±1.4, 22.6±2.5, 21.6±1.9, 18.3±1.5, 17.4±1.7, respectively. At the maximal % NC site from segment 1 to 5, the necrotic core percentage was 28.1±2.3, 38.5±3.7, 37.7±3.8, 30.3±3.1, 29.6±2.2, respectively. Multiple comparison results showed that the fibrous tissue percentage of segment 2 and 3 was significantly lower than that of the other segments and the % NC was significantly higher than that of the other segments. The differences were statistically significant (p<0.05). Analytical results of contralateral bifurcation ridge plaques were: fibrous tissue percentage was 41.1±2.2, fibrous lipid tissue percentage was 4.2±0.9, calcified tissue percentage was 21.6±1.9, % NC was 34.3±2.7. The analytical results of bifurcation ridge plaques were: fibrous tissue percentage was 51.6±2.6, fibrous lipid tissue percentage was 6.0±0.6, calcified tissue percentage was 14.2±1.1, % NC was 29.2±2.2. The contralateral bifurcation ridge had lower fibrous tissue percentage and higher % NC than the bifurcation ridge; the differences were statistically significant (p<0.05) (Figures 4 and 5).

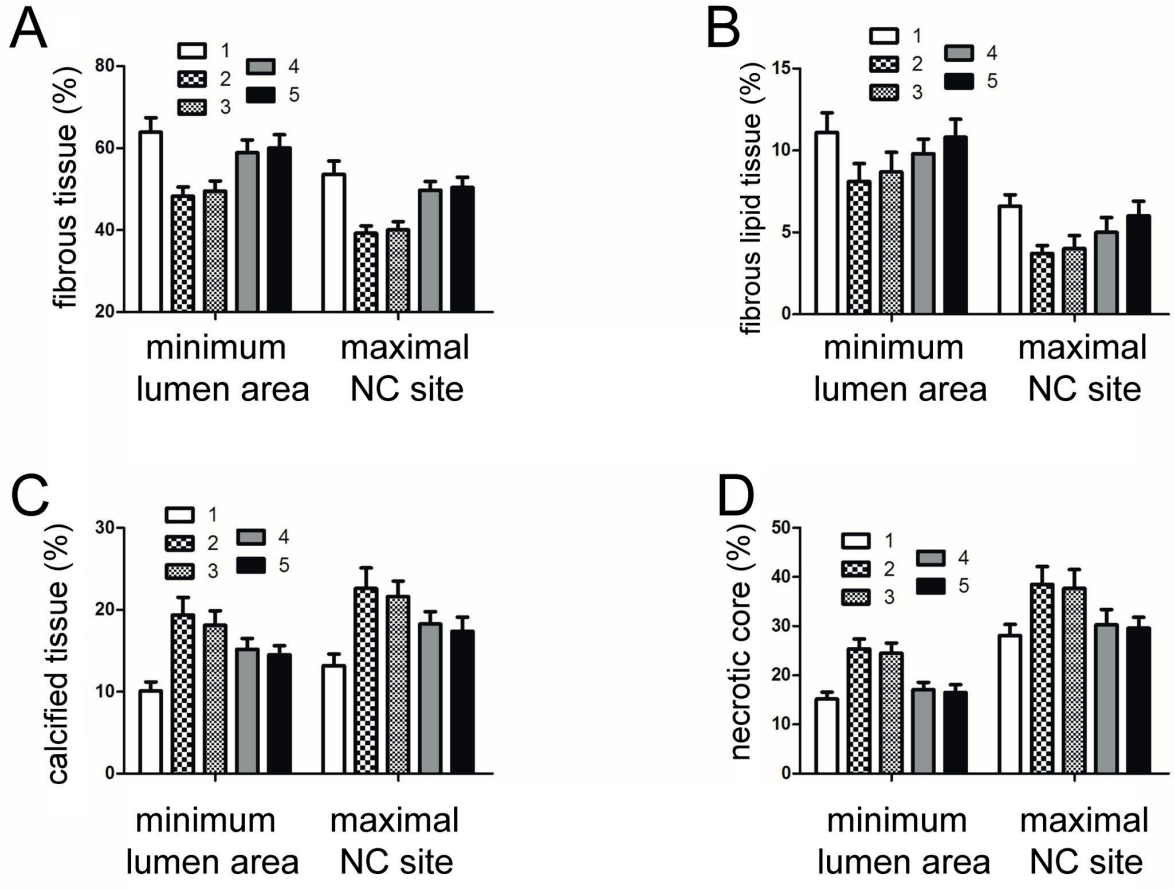

Figure 4. Analysis of plaque tissue structure of the 5 segments in the LMCA bifurcation at the minimum lumen area site and the maximal % NC site. ***A,*** Fibrous tissue; ***B,*** Fibrous lipid tissue; ***C,*** Calcified tissue; ***D,*** Necrotic core. Intravascular ultrasound showed, at the minimum lumen area site and the maximal % NC site, the fibrous percentage of segment 2 and 3 in left main bifurcation was significantly lower than that of the other segments, the % NC was significantly higher than that of the other segments.

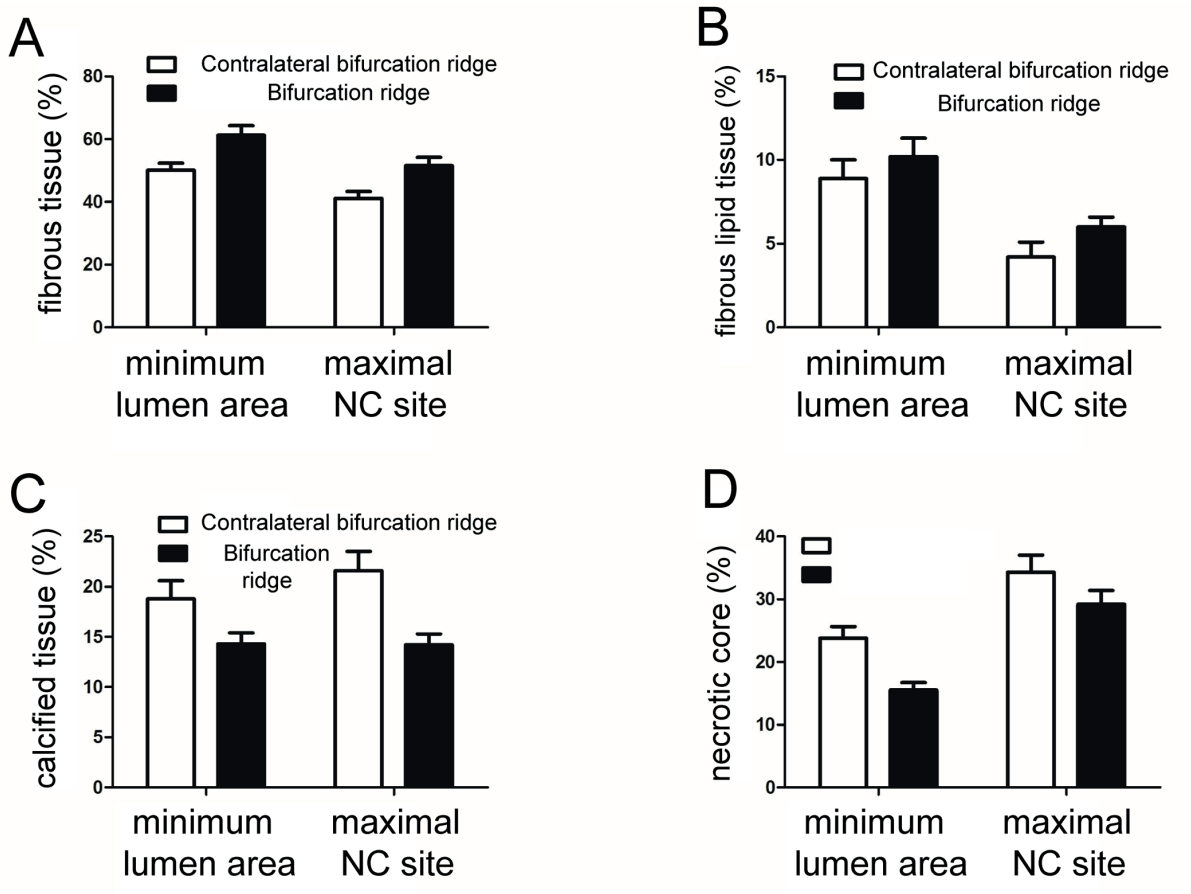

Figure 5. Analysis of plaque tissue of the left main bifurcation ridge and the left main contralateral bifurcation ridge at the minimum lumen area site and the maximal % NC site. ***A,*** Fibrous tissue; ***B,*** Fibrous lipid tissue; ***C,*** Calcified tissue; ***D,*** Necrotic core. Intravascular ultrasound showed, at the minimum lumen area site and the maximal % NC site, the fibrous percentage of the contralateral bifurcation ridge was significantly lower than that of the bifurcation ridge, the % NC was significantly higher than that of the bifurcation ridge.

Discussion

The atherosclerotic plaques occur more frequently at the site of arterial bifurcation. The reason is due to changes in blood flow patterns. A simple axial blood flow through the arterial bifurcation produces turbulence, which further impacts on the blood vessel wall and leads to lower the shear stress along the main blood branch. The shear stress at the lateral wall of side branch and the distal end was high, while it was low at the side branch ostium, proximal part, and the contralateral bifurcation ridge. The shear stress at the bifurcation ridge was the highest[10]. The difference in shear stress directly affects the distribution and characteristics of atherosclerotic plaques in the coronary artery bifurcation and the plaque always distributes from low shear stress to high shear stress[11,12]. The plaques at a higher shear stress site are usually derived from plaques at a lower shear stress site. In this study, we found that the plaques at the bifurcation lesion of ostium and proximal end had heavier burdens than at the distal end; plaques at the contralateral bifurcation ridge had heavier burdens than at the bifurcation ridge. These results were found to be similar to the results of previous studies[13,14]. The difference in the distribution of plaque and shear stress can affect the endothelial function[15,16]. The endothelium under the shear stress can produce histamine, prostacyclin, and other substances[15], which causing the dilation of blood vessels, inhibition of platelet aggregation, synthesis, secretion of fibrinolytic activators, and the inhibition of thrombosis. Many antithrombotics secreted by the endothelium are shear stress-dependent[16] and shear stress can affect the differentiation, maturation, and aggregation of adipocytes[17]. However, in

the low shear stress area, the endothelium showed limited function, which is easy to cause the formation and rupture of atherosclerotic plaques[18,19]. The rupture of unstable plaques is the main mechanism of acute coronary artery syndrome and introduces the sudden cardiac death[20]. Previous researches[21,22] found that the main morphological features before the rupture of plaque were the thinning of the fiber cap, larger necrotic core and the large amounts of fat necrotic tissue in the core. We found that the plaques, which were located at the sites of bifurcation ostium and the proximal end of the bifurcation lesion, had lower fibrous tissue components, higher % NC, suggesting higher vulnerability to rupture, which is consistent with previous studies and clinical findings. In patients with acute coronary syndromes, a majority of patients had stenosis or occlusion at the ostium or proximal end of the main branch bifurcation[23]. Clearing plaques at bifurcation sites may contribute to further interventional therapy[24,25].

Our work was a single-center study with a small sample size. Therefore, there will be a need for further research with multi-center, large sample, randomized control studies to confirm the results.

Conclusions

This study demonstrated that IVUS performed in interventional therapy can clear the characteristics and composition of coronary atherosclerotic plaque; therefore, it clarifies the stability of the plaque since the instability of plaque is a major factor in cardiovascular incidents. Therefore, this work demonstrated the necessity of IVUS application in interventional therapies. According to our results, we can initially determine the characteristics of plaques at different LMCA bifurcation sites, which can provide a primary guidance for interventional therapy if there is no condition to perform IVUS.

Conflict of Interest

The Authors declare that they have no conflict of interest.

References

1) Chieffo A, Hildick-Smith D. The European Bifurcation Club Left Main Study (EBC MAIN): rationale and design of an international, multicentre, randomised comparison of two stent strategies for the treatment of left main coronary bifurcation disease. Eurointervention 2016; 12: 47-52.
2) Ragosta M. Left main coronary artery disease: importance, diagnosis, assessment, and management. Curr Probl Cardiol 2015; 40: 93-126.
3) Cheng CI, Lee FY, Chang JP, Hsueh SK, Hsieh YK, Fang CY, Chen SM, Yang CH, Yip HK, Chen MC, Fu M, Wu CJ. Long-term outcomes of intervention for unprotected left main coronary artery stenosis: coronary stenting vs coronary artery bypass grafting. Circ J 2009; 73: 705-712.
4) Martinez GJ, Molina J, Byrom M, Puranik R, Ng B, Bailey BP, Patel S, Dworakowski R, MacCarthy P, Ochala A, Smolka G. How should I treat a complex critical left main bifurcation lesion in a patient with poor left ventricular function, an occluded dominant right coronary artery and severe peripheral vascular disease? Eurointervention 2015; 11: 485-488.
5) Jin ZG, Zhang ZQ, Jing LM, Wei YJ, Zhang J, Luo JP, Yang SL, Ma DX, Liu Y, Han W, Yang Y, Liu HL. Correlation between dual-axis rotational coronary angiography and intravascular ultrasound in a coronary lesion assessment. Int J Cardiovasc Imaging 2017; 33: 153-160.
6) Xu J, Hahn JY, Song YB, Choi SH, Choi JH, Lu C, Lee SH, Hong KP, Park JE, Gwon HC. Carina shift versus plaque shift for aggravation of side branch ostial stenosis in bifurcation lesions: volumetric intravascular ultrasound analysis of both branches. Circ Cardiovasc Interv 2012; 5: 657-662.
7) Kang SJ, Kim WJ, Yun SC, Park DW, Lee SW, Kim YH, Lee CW, Park SW, Mintz GS, Park SJ. Vascular remodeling at both branch ostia in bifurcation disease assessed by intravascular ultrasound. Catheter Cardiovasc Interv 2013; 81: 1150-1155.
8) Yazici HU, Agamaliyev M, Aydar Y, Goktekin O. The impact of intravascular ultrasound guidance during drug eluting stent implantation on angiographic outcomes. Eur Rev Med Pharmacol Sci 2015; 19: 3012-3017.
9) Kang SJ, Mintz GS, Kim WJ, Lee JY, Park DW, Yun SC, Lee SW, Kim YH, Lee CW, Han KH, Kim JJ, Park SW, Park SJ. Effect of intravascular ultrasound findings on long-term repeat revascularization in patients undergoing drug-eluting stent implantation for severe unprotected left main bifurcation narrowing. Am J Cardiol 2011; 107: 367-373.
10) Gerhold KA, Schwartz MA. Ion channels in endothelial responses to fluid shear stress. Physiology (Bethesda) 2016; 31: 359-369.
11) Wang Y, Qiu J, Luo S, Xie X, Zheng Y, Zhang K, Ye Z, Liu W, Gregersen H, Wang G. High shear stress induces atherosclerotic vulnerable plaque formation through angiogenesis. Regen Biomater 2016; 3: 257-267.
12) Browne LD, Bashar K, Griffin P, Kavanagh EG, Walsh SR, Walsh MT. The role of shear stress in arteriovenous fistula maturation and failure: a systematic review. PloS One 2015; 10: e145795.

13) Chang M, Kang SJ, Yoon SH, Ahn JM, Park DW, Lee SW, Kim YH, Lee CW, Park SW, Nakazawa G, Mintz GS, Park SJ. Plaque composition and morphologic characteristics in significant left main bifurcation disease; virtual histology intravascular ultrasound study. Coron Artery Dis 2016; 27: 623-628.

14) Li L, Dash D, Gai LY, Cao YS, Zhao Q, Wang YR, Zhang YJ, Zhang JX. Intravascular ultrasound classification of plaque in angiographic true bifurcation lesions of the left main coronary artery. Chin Med J (Engl) 2016; 129: 1538-1543.

15) Chistiakov DA, Orekhov AN, Bobryshev YV. Effects of shear stress on endothelial cells: go with the flow. Acta Physiol (Oxf) 2017; 219: 382-408.

16) Baeyens N, Bandyopadhyay C, Coon BG, Yun S, Schwartz MA. Endothelial fluid shear stress sensing in vascular health and disease. J Clin Invest 2016; 126: 821-828.

17) Choi J, Lee SY, Yoo YM, Kim CH. Maturation of adipocytes is suppressed by fluid shear stress. Cell Biochem Biophys 2017; 75: 87-94.

18) Wong WT, Ma S, Tian XY, Gonzalez AB, Ebong EE, Shen H. Targeted delivery of shear stress-inducible micrornas by nanoparticles to prevent vulnerable atherosclerotic lesions. Methodist Debakey Cardiovasc J 2016; 12: 152-156.

19) Cao XQ, Liu XX, Li MM, Zhang Y, Chen L, Wang L, Di MX, Zhang M. Overexpression of Prolyl-4-Hydroxylase-alpha1 stabilizes but increases shear stress-induced atherosclerotic plaque in apolipoprotein E-Deficient mice. Dis Markers 2016; 2016: 1701637.

20) Sanchis-Gomar F, Perez-Quilis C, Leischik R, Lucia A. Epidemiology of coronary heart disease and acute coronary syndrome. Ann Transl Med 2016; 4: 256.

21) Gao H, Long Q, Graves M, Gillard JH, Li ZY. Carotid arterial plaque stress analysis using fluid-structure interactive simulation based on in-vivo magnetic resonance images of four patients. J Biomech 2009; 42: 1416-1423.

22) Liu K, Hua BT, Guo T, Pu LJ. The assessment of the long-term effects of elective CRT-D of coronary heart disease after PCI. Eur Rev Med Pharmacol Sci 2017; 21: 1313-1317.

23) Salvagno GL, Pavan C. Prognostic biomarkers in acute coronary syndrome. Ann Transl Med 2016; 4: 258.

24) Niemela M, Kervinen K, Erglis A, Holm NR, Maeng M, Christiansen EH, Kumsars I, Jegere S, Dombrovskis A, Gunnes P, Stavnes S, Steigen TK, Trovik T, Eskola M, Vikman S, Romppanen H, Makikallio T, Hansen KN, Thayssen P, Aberge L, Jensen LO, Hervold A, Airaksinen J, Pietila M, Frobert O, Kellerth T, Ravkilde J, Aaroe J, Jensen JS, Helovist S, Sjogren I, James S, Miettinen H, Lassen JF, Thuesen L. Randomized comparison of final kissing balloon dilatation versus no final kissing balloon dilatation in patients with coronary bifurcation lesions treated with main vessel stenting: the Nordic-Baltic bifurcation study III. Circulation 2011; 123: 79-86.

25) Chen SL, Santoso T, Zhang JJ, Ye F, Xu YW, Fu Q, Kan J, Paiboon C, Zhou Y, Ding SQ, Kwan TW. A randomized clinical study comparing double kissing crush with provisional stenting for treatment of coronary bifurcation lesions: results from the DKCRUSH-II (Double Kissing Crush versus Provisional Stenting Technique for Treatment of Coronary Bifurcation Lesions) trial. J Am Coll Cardiol 2011; 57: 914-920.